

PLANETARY TERRAIN ANALYSIS FOR ROBOTIC MISSIONS

V. Masarotto, L. Joudrier, J. Hidalgo Carrio, and L. Lorenzoni

ESA/ESTEC, (NETHERLANDS)

ABSTRACT

From the early studies to the actual design of a planetary rover mission, the knowledge of the type of terrain that will be encountered is crucial. Usually, a reference terrain is defined to help the design of the rover subsystems, knowing that the terrain will be different during the actual mission. Furthermore, once the landing site is selected, the evaluation of the slopes is essential to measure the performance of an Entry, Descent and Landing System.

The main goal of this paper is exposing the method used to measure the slopes distribution of a terrain from its Digital Elevation Maps and, through this, explain the requirements set for the reference terrain for Mars mission. At the end, there are presented methods to generate sample terrains to be used for rover design and navigation verification.

1. ADIRECTIONAL SLOPE METHOD

In order to proceed with the mission design, it is fundamental to have an idea of the terrain on which the rover is going to land. To evaluate the performance of an EDL system, it is crucial to have a measurement of the slopes for the baselength of interest, while rover missions need a detailed knowledge of the terrain for navigation on-site and for rover's development and testing. Since knowledge *a priori* of the terrain is not possible in general, an accurate simulation is crucial for the evaluation of the mission performance..

For the generation of the reference terrain, ESA has defined requirements for various missions like the ExoMars rover, the EDL demonstrator or the Mars Sample Fetching Rover study.

The primary parameters associated with DEM which describe terrain surfaces are slopes, aspects and rocks. While the rocks distribution law has been defined and verified over several places on Mars by Golombek et al [G03], the slopes studies never output an model to be used for terrains generation.

In this section two different algorithms to compute slopes are presented. In particular it is defined and explained a new slopes measurement method, the so-called Adirectional Slope Method (ASM).

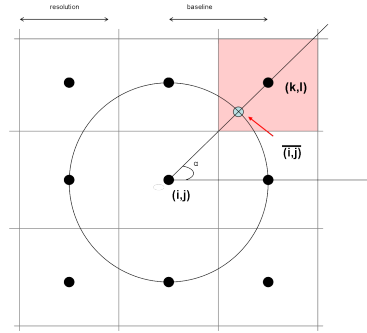


Figure 1. Visual description for ASM.

It is also given an analysis via ASM of some landing site candidates for MSL.

1.1. Adirectional Slope Method

Def. The adirectional slope in a point is given by the absolute value of the maximum slope computed around the point, measured at a specific length scale.

To compute the adirectional slopes of a given DEM, the statistic software R [R] has been used.

The Adirectional Slope Method ASM works as follows (see Figure 1 for a visual description): set a baselength L and an increment angle α . For each point $P_{i,j}$ of the DEM, consider a circular window of radius L centred in $P_{i,j}$. For every point $\bar{P}_{i,j}$ identified by the increments of width α on the circumference, ASM searches for the point $P_{k,l}$ on the DEM which is the closest one to $\bar{P}_{i,j}$ and calculates the slope between $P_{k,l}$ and the centre of the circle $P_{i,j}$. Finally it associates to the $P_{i,j}$ the maximum slope value.

The angle α and the baselength L both depend on the resolution of the DEM. As a general guideline, $\alpha = 15^\circ$ is a good value for the angle, while, if possible, for the baselength it is recommended to pick L greater than the DEM resolution.

A high level description of the algorithm is given by:

```

numPoints = 2π/α
for i = 0 until number of columns on DEM
  for j = 0 until number of rows on DEM
    for n = 0 until numPoints
      k = round[i + (L/resolution) cos(nα)]
      l = round[j + (L/resolution) sin(nα)]
      distance = dist[(i, j), (k, l)]
      slope(n) = arctan((z(i, j) - z(k, l))/dist)
    slopes(i, j) = max(slope)
  
```

1.2. Steepest Neighbour

The Steepest Neighbour method (SN) is a slopes computation method already presented in literature (see [Gu95]).

Let the radius L be equal to the resolution of the DEM. SN picks the steepest slope among the eight adjacent points to $P_{i,j}$, considering the real distance on the grid, i.e. considering that the diagonal distance is longer and that vertical and horizontal spacings might be different from each others. The value is then assigned to the central point.

SN can be extended to larger values of L considering the 8 points as in Figure 2 (b).

While ASM and SN coincide when L equals the DEM resolution (they consider the same set of 8 points), at large base scales (e.g. 100m) SN misses a number of higher slopes, systematically minimizing the adirectional slopes value.

As it is recommended to use a base scale much higher than the DEM resolution, SN is not recommended to be used as a slopes computation method.

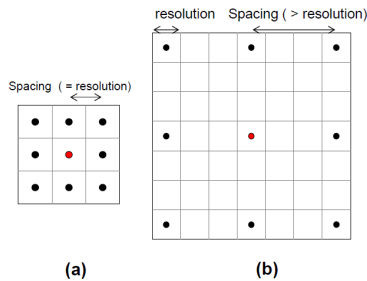


Figure 2. Steepest neighbour for L =resolution (in (a)) and $L > resolution$ (in (b)).

2. REQUIREMENTS FOR THE REFERENCE TERRAIN

In this section are presented the results obtained by applying ASM to the Mars Hi-Resolution DEM of four potential landing sites for MSL. The terrains available can be downloaded in the USGS Planetary GIS Web Server - PIGWAD ¹.

¹<http://webgis.wr.usgs.gov/ftphirise/>

All the DEMs are built via the HiRISE stereo cameras onboard the Mars Reconnaissance Orbiter and have a resolution of 1m. In order to cope with computer memory limitations though, the DEMs have been sampled to 5 meters resolution.

In Section 3 it is shown that these resamplings do not affect significantly the assumptions made on the terrains in terms of difficulties and slopes distribution.

Note that at 5m resolution the roughness induced by rocks and irregularities of the terrain are mostly smoothed out. Rocks though, do not have an impact on slopes computation as long as navigability is concerned, since they can be avoided by the rover.

As a consequence in particular, even the reference terrain can be given with a resolution of 1m, and at a later stage it can be refined through interpolation techniques and the rocks distribution model can be added (cfr. Section 4).

The four landing sites analysed in this document with essential information for ExoMars project are:

- Gale Crater;
- Holden Crater;
- Mawrth Vallis Landing site 2;
- Mawrth Vallis Landing Site 4.

The analysis of the DEMs is done importing the geo reference files on the Geographical Information System (GIS) GRASS ([GRASS]), and successively running the adirectional slope algorithm on the statistical environment R ([R]).

Latitude and longitude of the four landing site candidates	
Gale Crater:	min.latitude: -4.6757241932102 max.latitude: -4.2514300655544 westernmost long: 137.4239807 easternmost long: 137.5664978
Holden Crater:	min.latitude: -26.4688633214514 max.latitude: -26.0707102512555 westernmost long: 324.8796082 easternmost long: 325.0280762
Mawrth Vallis site 2:	min.latitude: -26.4688633214514 max.latitude: -26.0707102512555 westernmost long: 324.8796082 easternmost long: 325.0280762
Mawrth Vallis site 4:	min.latitude: 24.6346322372157 max.latitude: 25.0815451539359 westernmost long: 339.4687195 easternmost long: 339.6321106.

Figure 3 depicts the four images for these sites on Mars.

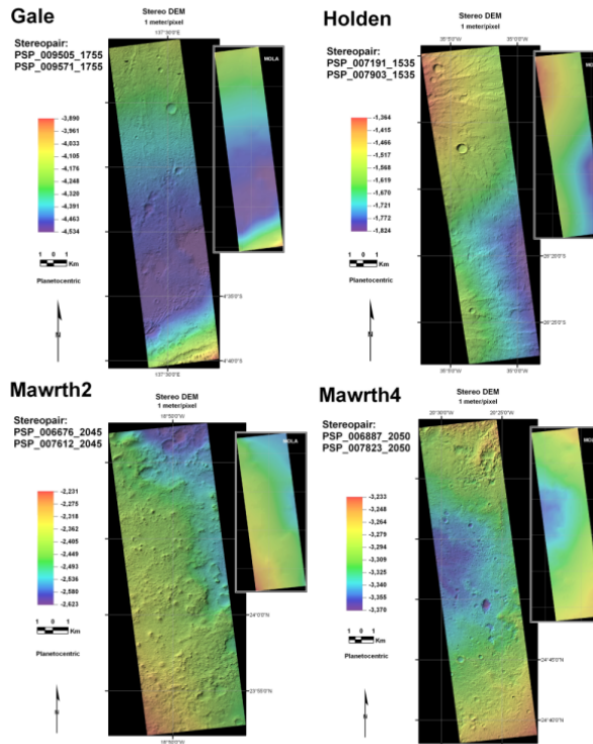


Figure 6 Mars HiRISE Hi-Resolution Topography of four possible landing sites

Figure 3. Candidates landing sites.

ESA focused on slopes computed over 5m and 100m distance. The assumption was made as well that over 5m, the terrain is fairly flat.

The objective was to define a known probability density function at 5m and at 100m that would enclose the difficulties of the four candidate landing sites of MSL. The model aimed to be used for describing a reference terrain to be used for navigation and system design.

2.1. Slopes distribution over 5m

Figure 4 shows that, although the slopes distributions over the four terrain are quite different from each other, they do carry some similar features, namely, the average slope and the behaviour towards higher slopes.

As a probabilistic model to describe the slopes behaviour, a Chi-square distribution of mean 7 seems to be a good match, of course accounting on some margin. The Chi-square density in fact resembles the shapes of the slopes density of the four terrains, being more conservative especially on low slopes. Since slopes higher than 20° are rare and can be avoided by the rover while travelling, low slopes are the most relevant for navigation. In particular, it is meaningful to stop at the Chi-square value of 21.5° for the 99.7th percentile for the reference terrain, although it is lower than the real terrains values.

Slopes values at the 99.7th percentile	
Gale Crater	37.54
Holden Crater	20.12
Mawrth2	31.47
Mawrth4	26.06
Chisq	21.5

2.2. Slopes distribution over 100m

At 100m scale, a Rayleigh distribution with parameter value of 3.5 seems to offer the best match. At this base-length, the slopes of the four terrains lose their common patterns, so the Rayleigh has been chosen for its conservativeness, as 75% of the slopes for the four analysed terrains stay below the third Rayleigh' quartile:

Slopes values at the third quartile	
Gale Crater	4.67
Holden Crater	3.51
Mawrth2	5.48
Mawrth4	3.2
Rayleigh	5.82

Figure 5 compares the slopes density distribution of the four terrains against the Rayleigh distributions. Ob-

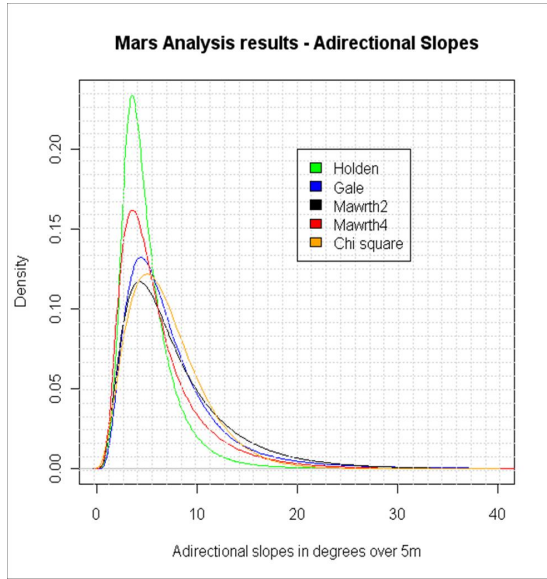


Figure 4. Slopes distribution for the four landing sites compared with Chisq.

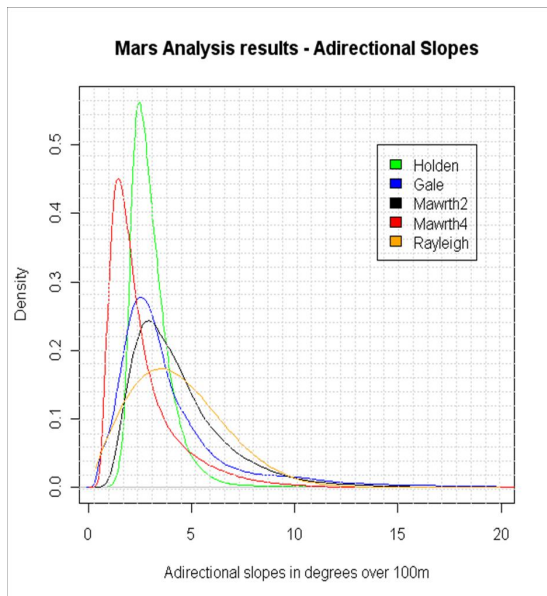


Figure 5. Slopes distribution for the four landing sites compared with Rayleigh.

serve that Gale and Mawrth2 present higher slopes than the chosen Rayleigh model, as it is showed in the table

Slopes values at the 99.7th percentile	
Gale Crater	21.5
Holden Crater	11.4
Mawrth2	14.5
Mawrth4	10.8
Rayleigh	12

These values though seem to correspond at specific restricted areas on the terrains (irregularities, craters), which should be avoided as much as possible when fitting the landing ellipse, and as well by the rover while travelling.

2.3. Summary

Here the summary of the requirements for the reference terrain:

Reference terrain requirements	
5m baselength	maximum slope (99.7th perc): 21.5° Chi-square distribution
100m baselength	maximum slope (99.7th perc): 12° Rayleigh distribution

3. COMPARISON BETWEEN 1M RESOLUTION AND 5M RESOLUTION

The analysis on Figure 6 and 7 have been performed on a 3km sub-DEM of Mawrth2 and Gale. On these sub-DEM, there is no significant difference between the computations performed with 5m and 1m resolution respectively.

This means that the selected subsets of the terrains are fairly smooth. The assumption is that the high frequencies of a terrain are provided by the rocks. Other larger hazards are not frequent and would be detected and avoided by the navigation system.

Note that for $L = 100m$ all the difference will be smoothed out by the division by L .

4. ROCKS DISTRIBUTION

From data of the Viking landing sites, *Golombek et Rapp, 1997* [G97] found that the size-frequency distribution of rocks could be fit with exponential functions. The cumulative fractional area covered by rocks of diameter greater than a given D is given by:

$$F(D) = k \exp(-q(k)D)$$

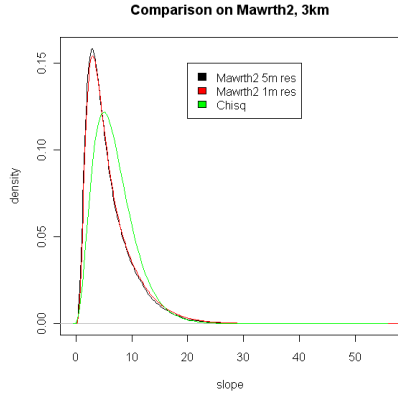


Figure 6. Comparison over a 3km sub-DEM of Mawrth2, 5m baselength.

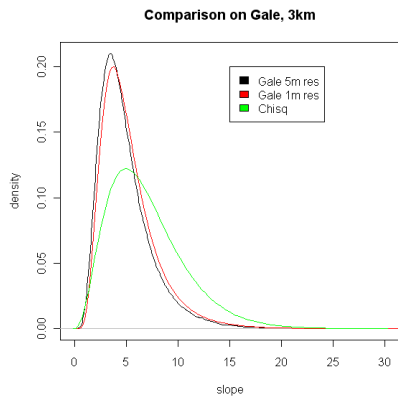


Figure 7. Comparison over a 3km sub-DEM of Gale, 5m baselength.

where k is the total rock coverage (estimated from thermal differencing techniques), $q(k)$ governs how abruptly the area covered by rocks decreases with increasing diameters and the average rock diameter D is the average of the horizontal length of the rock long axis and the horizontal length of the rock short axis (more correct than apparent width, see [G03] pg. 27-5,6).

The value $q(k)$ is empirically approximated by

$$q(k) = 1.79 + 0.152/k,$$

while for k ExoMars has been considering up to now 6.9% of rock abundance for its reference terrain, recognizing that on Mars we can find locally much higher rock abundance.

4.1. Cumulative number of rocks

Many engineering applications prefer the cumulative number of rocks with diameter greater than D , rather than the cumulative area covered by them.

The cumulative number of rocks for m^2 larger or equal

than a given diameter can be derived via numerical integration of the cumulative fractional area, i.e.

$$N(D) = \int_D \frac{F}{\text{area}}.$$

Now, given the total rocks coverage and the cumulative fractional area, $N(D)$ gives rise to a deterministic model. But for modelling purposes the rocks are thought to be distributed probabilistically on the surface, and it is needed to know which is the probability of having n rocks of a given diameter over a given area. Golombek *et al.* deduced in [G03] that rocks are scattered over a surface according to a Poisson distribution. In particular the probability of having n rocks over a surface of area S is given by a homogeneous 2-dimensional Poisson spatial process of mean $N \times S$, i.e.

$$p_{S,N}(n) = \frac{N^n S^n}{n!} \exp(-NS).$$

Note that assuming that the Poisson process is homogeneous implies that the mean $N \times S$ is not a function of the position. In particular clusters or clumping are not considered.

It follows that the probability that at least one rock of a specified size is inside S is given by

$$1 - p_{S,N}(0) = 1 - \exp(-NS).$$

Finally, generating a Poisson field over a surface S is straightforward: for every finite covering $(A_i)_i$ of S , compute the Poisson number of rocks and then scatter the points uniformly over each A_i . Since this holds for every finite covering, it holds in particular for the all surface S . Note the program "R" provides all the functions to distribute the rocks over the terrain according to poisson distribution.

5. REFERENCE TERRAIN

In recent years, generating realistic looking terrain has been a point of interest for computer graphic specialists, video-games creator, geologist and other scientists, therefore various software for terrain generation have been launched on the market, most of which are based on predefined real terrain or on fractal models. In our case the main goal was generating a terrain which was not only realistic, but mainly compatible with the ESA requirements on slopes distribution described in Section 2.

Various methods have been investigated, from the most trivial one of interpolate random values scattered over a plane to more complex ones. The following Section provides a short description of the attempts that seemed more relevant.

Rocks distribution according to Section 4 has been added on a second stage, and was not involved in slopes computation.

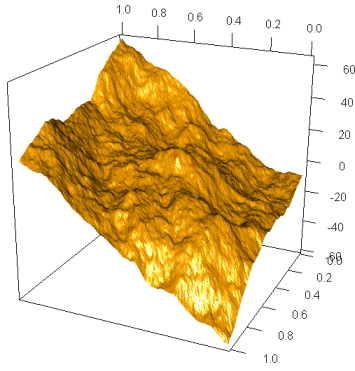


Figure 8. Terrain generated via Variogram model, 50cm resolution, 570m×570m, with rocks.

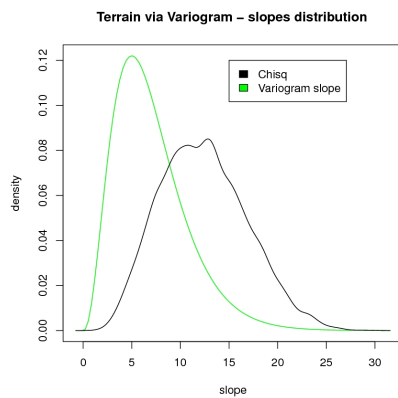


Figure 9. Slopes analysis of the terrain generated via Variogram.

5.1. Terrain generation via Variograms

One of the most widely used tool for investigating the structure of spatial data is the semivariogram (or variogram), which measures the average dissimilarity of the data over a given area.

Variograms can be used to generate two-dimensional random fields². The idea is the following: compute a variogram model from a Mars real terrain, then use the variogram and kriging techniques the data at specific grid location and generate different terrains which all have the same (adirectional) variogram. In this way all the new realisations should preserve the behaviour over the close or far field.

There are several parameters to play with while generating a random field, but in general the statistical distribution of the slopes is not preserved in the process. Figures 8 and 9 show one of the best result obtained.

²R offers the package RandomFields to generate random fields via variogram

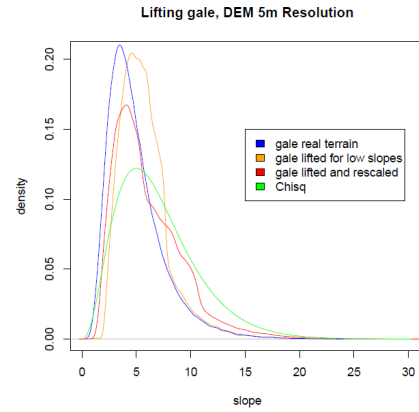


Figure 10. Manual modification of Mawrth2 DEM, 5m resolution. Scaling factor: 1.4. Lifting parameter: 0.5m.

5.2. DEM modifications: rescaling and lowering

It is possible to intervene manually on a DEM to modify the slope distribution. We have investigated two possible techniques to 'lower' the curve of the slope density and shifting it to the right, producing thus a terrain with a larger amount of higher slopes.

The first technique ("rescaling") fixes a reference height h , say the mean of the heights of the terrain, and multiply all the height values higher that h by a constant factor while dividing all the height values lower than h by the same factor. This procedure give rise to a bigger amount of larger slopes, i.e. lowers the slopes density curve.

The second technique ("lowering"), identifies all the points where the adirectional slope is less than a pre-determined parameter s and lower the DEM in these points by a fixed constant amount. In this way, part of the lower slopes will disappear and the slopes density curve will be shifted to the right.

Figure 10 shows the result of applying these two procedures on Gale Crater, while Figures 12 and 13 show a modified fractal terrain and its slopes distribution.

Note that, by modifying the parameters, is possible to obtain different slopes distributions.

5.3. Fractal terrain

Real landscape features like rocks or mountains or coastlines can show a fractal behaviour, in particular they are self-similar (i.e. the overall shape is resembling the shape of one or more of their parts) and do have a fractal dimension. As a consequence fractal based terrain generation techniques can produce very realistic result and are therefore widely used. Moreover, fractal algorithms are fast and in general easy to implement.

The fractal terrain generator presented in this paper is a 3D-implementation of the midpoint displacement algorithm. The algorithm starts with a 2x2 matrix of randomly generated terrain heights, namely the coordinates of the vertexes of a square on a plane, then iteratively

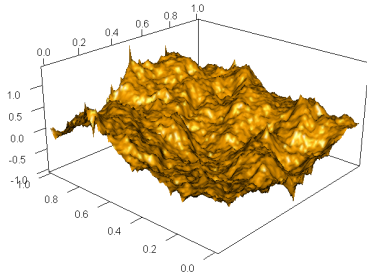


Figure 11. Terrain generated via fractal model, 50cm resolution, 129m×129m, with rocks.

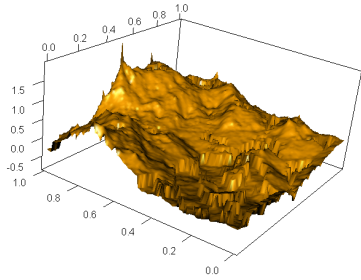


Figure 12. Fractal terrain modified. Scaling factor: 1.4, lowering parameter: -0.3. The jumps are due to the rescaling and can be smoothed.

it subdivides the square into four sub-squares and assigns proper values to each of the new vertex (namely, the mean of adjacent knots). Then it calls itself repetitively.

This algorithm indeed gives rise to realistically looking terrain, but due to the randomness of the parameter, it is not eligible as a general method to give a reference terrain compatible with the requirements.

In general, slopes distribution for a fractal terrain tend to underestimate greatly the Chi-square.

Figures 11 show an example of the terrain. Its slope distribution can be seen in 13 (along with the slope density curves of the terrain modified according to Sub-

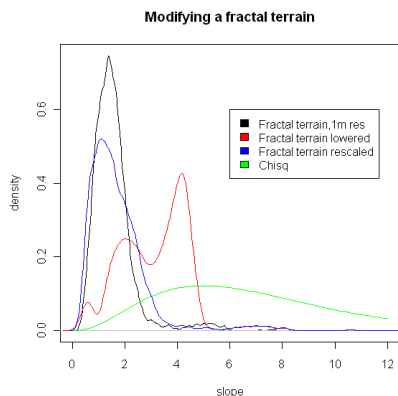


Figure 13. Slopes analysis of the modified fractal terrain. Scaling factor: 1.4, lowering parameter: -0.3.

section 5.2).

Note that the slopes distribution might be improved re-generating the terrain, or can be modified manually as in Sub-section 5.2 (see Figures 12 and 13).

5.4. Manual terrain generation

Another attempt to generate the terrain was done generating a DEM point by point.

Assume the baselength L is equal to 5 and set the height of an initial set of points. For every point $P_{i,j}$ belonging to the set, the slope between $P_{i,j}$ and $P_{k,l}$ must satisfy the two following conditions:

1. $\text{slope}_{(i,j),(k,l)} \in \chi^2$ (risp. Rayleigh),
2. $\text{slope}_{(i,j),(k,l)} < \text{maximum slope}$.

Thus, pick random Chi-square deviates from a Chi-square distribution of mean 7 and define the heights of all the points distant L from $P_{i,j}$ such that the slopes equal such deviates. Then repeat for every point.

While iterating the algorithm, special care must be put on the fact that the heights of every new point at distance L , say $P_{i,j} + L$, not only must satisfy all the slope conditions relative to $P_{i,j}$, but also to all the points of the kind $P_{i,j} + 2L$, i.e. points distant L from $P_{i,j} + L$ itself.

This care translates into a too numerous amount of conditions to be written for every point of the DEM though. For this reason, given $P_{i,j}$, the algorithm has been simplified moving only "vertically" and "horizontally" on the grid, i.e. for every $P_{i,j}$, we only generated the heights $P_{i+L,j}$ and $P_{i,j+L}$.

Note. Let P_i , $i = 1, \dots, 5$ be 5 points of a DEM arranged like in Figure 14. Assume P_1 to be given and P_2 , P_3 be generated from P_1 during the first step of the algorithm and move to P_2 to iterate the algorithm, generating thus the heights of P_4 and P_5 . It is needed that the slope between P_2 and P_4 satisfies the conditions (1.) and (2.) above.

Call z_i the height of P_i , then:

$$|z_3 - z_4| < |z_3 - z_1| + |z_1 - z_2| + |z_2 - z_4| = \text{dist}(\tan \text{slope}_{1,3} + \tan \text{slope}_{1,2} + \tan \text{slope}_{2,4}).$$

Thus if $\text{slope}_{2,4}$ is taken to be a Chi-square deviate such that

$$\tan(\text{slope}_{2,4}) = \tan(\text{slope max}) - \tan(\text{slope}_{1,3}) - \tan(\text{slope}_{1,2}) \quad (1)$$

then the conditions will be satisfied.

A high level description of the algorithm in this case is given by:

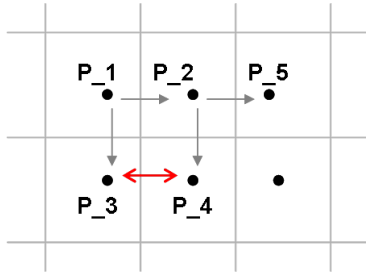


Figure 14. Algorithm for manual terrain generation.

```

slope_vector ← vector of random chisq(7) deviates
for i = 0 until number of columns on DEM
for j = 0 until number of rows on DEM
  if slope(i,j),(i+L,j) does not satisfies (1)
    recompute random deviate
  else
    zi+L,j+L = zi,j + dist × slope(i,j),(i+L,j)
    zi,j+L = zi,j + dist × slope(i,j),(i,j+L)

```

This procedure though generates a terrain which satisfy the slopes distributions, but it looks "folded". For this reason the DEM has been manually smoothed to obtain finally the terrain in Figure 15.

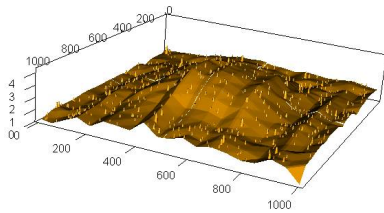


Figure 15. Manually generated terrain, 10cm resolution, 100m×100m, with rocks. The height coordinate has been rescaled to make the change in altitude more apparent.

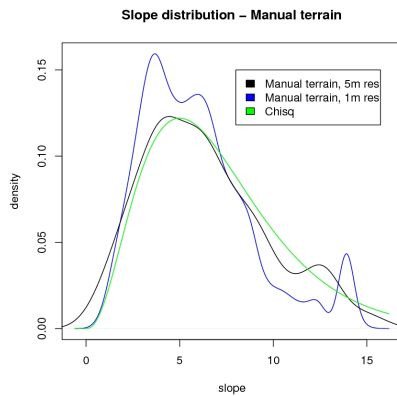


Figure 16. Slopes analysis of the terrain generated via manual method that gave the closest result to the requirements.

6. CONCLUSIONS

A method to compute adirectional slopes has been proposed and used to define reference distributions for design of martian rover missions like ExoMars rover or Mars Sample Fetching Rover. Various methods to generate a terrain satisfying the requirements have been tried with limited success. Now that we have gained experience in the statistical tool "R", future work will focus on automating the manual process.

REFERENCES

- [G03] Golombek, M. P., et al., 2003, Rock size-frequency distributions on Mars and implications for MER landing safety and operations: J. Geophys. Res., v. 108(E12), 8086, doi:10.1029/2002JE002035, 23pp.
- [G97] Golombek, M., and Rapp, D., 1997, Size-frequency distributions of rocks on Mars and Earth analog sites: Implications for future landed missions: J. Geophys. Res., v. 102, p. 4117-4129.
- [Gu95] Guth, P.L., 1995. Slope and aspect calculations on gridded digitalelevation models: examples from a geomorphometric toolbox for personal computers. Zeitschrift fu r Geomorphologie N. F., Supplementband 101, 31e52.
- [GRASS)] <http://grass.fbk.eu/>
- [R] <http://cran.r-project.org/>